

Numerical Investigation Using Harmonic and Transient Analysis To Rotor Dynamics

Prof. Adnan Naji Jameel Al Tamimi
Department of Mechanical Engineering
College of Engineering
University of Baghdad
Email: adnanaji2004@yahoo.com

Ph.D. Student. Jassim Farij Thiheel Al Draji
Department of Mechanical Engineering
College of Engineering
University of Baghdad
Email: jassim_aldrajy@yahoo.com

ABSTRACT

The rotor dynamics generally deals with vibration of rotating structures. For designing rotors of a high speeds, basically its important to take into account the rotor dynamics characteristics. The modeling features for rotor and bearings support flexibility are described in this paper, by taking these characteristics of rotor dynamics features into standard Finite Element Approach (FEA) model. Transient and harmonic analysis procedures have been found by ANSYS, the idea has been presented to deal with critical speed calculation. This papers shows how elements BEAM188 and COMBI214 are used to represent the shaft and bearings, the dynamic stiffness and damping coefficients of journal bearings as a matrices have been found with the variation of rotation speed of the rotor which are vary with eccentricity of journal with bearings and this eccentricity is a function of Sommerfeld number, the first critical speed analysis has been done from Campbell diagram, the critical speed it is the speed at which resonance case happen, the unbalance response analysis has been done with changing the unbalance mass then finding the maximum response of the rotor for each unbalance mass case, by Campbell diagram plot recognizing the stability of the system and find the line of un stability, above and down this line the system is stable and if speed lies on this line the system is unstable, the main reason of analysis of rotor dynamics is to help Engineers to characterize the lateral dynamics characteristics of a given design with Campbell diagram plot, can find the critical speed, the unbalance response and the system stability .

Key words: rotor dynamics, critical speed, unbalance response, stability

دراسة عددية للتحليل الحركي المتناسق والوقتي للمحور الدوار

طالب دكتوراه. جاسم فرج ثجيل الدراجي
قسم الهندسة الميكانيكية
كلية الهندسة / جامعة بغداد

استاذ. عدنان ناجي جميل التميمي
قسم الهندسة الميكانيكية
كلية الهندسة / جامعة بغداد

الخلاصة

ان حركة المحاور الدوارة بصورة عامة تتعامل مع اهتزازات الهياكل ، لغرض تصميم المحاور ذات السرعة العالية من المهم ان تأخذ بالحسبان الخصائص الحركية للمحور الدوار. ان مميزات تمثيل المحور مع المحامل ضمن المرونة قد درست في هذا البحث، وبأخذ هذه الخصائص عن طريق التحليل بواسطة الشريحة المحددة وقد وجدت طريقة للتحليل المتناسق والوقتي بواسطة ال ANSYS ، ان الفكرة الاساسية هي كيفية التعامل مع حسابات السرعة الحرجة وتم التبيان عن كيفية استخدام الشريحة نوع BEAM188 ونوع COMBI214 لتمثيل المحور الدوار والمحامل الهيدروليكية، ان النابضية والتخميد المتولدتان في المحامل نتيجة الحركة الدورانية كقيم مصفوفات تم ايجادها مع تغيير السرعة الدورانية والتي بدورها تتغير مع اللامركزية بين المحور والمحامل الذي يعمل معها وان هذه اللامركزية هي بالاساس دالة لرقم Sommerfeld، تم ايجاد السرعة الحرجة الاولى من مخطط Campbell وهي السرعة التي تحدث عندها حالة ال Resonance وكذلك تم ايجاد الاستجابة للمحور مع التغيير في كتلة عدم التوازن وايجاد اعلى استجابة لكل حالة من كتلة عدم التوازن وكذلك من خلال رسم مخطط Campbell تم تحديد منطقة الاستقرارية حيث ان المناطق اسفل واعلى الخط الافقي الاول هي مناطق استقرار حركي اما اذا وقعت على الخط فان النظام غير مستقر، ان السبب الرئيسي للتحليل

الحركي للمحور الدوار هو لمساعدة المهندسين لمعرفة خصائص الحركة العمودية على مركز محور الدوران وبوجود مخطط Campbell ممكن ان نعرف السرعة الحرجة، استجابة النظام بوجود كتلة عدم التوازن واستقرارية النظام الحركي.
الكلمات الرئيسية: حركة المحور، السرعة الحرجة، استجابة عدم الاتزان، الاستقرارية.

1. INTRODUCTION

Because the rotors are wide used in industry like steam turbines, gas turbines, fans and stator of electric motors. The growth in power and more difficult design of turbomachines accompanied by higher requirements to their reliability. To increase the life of rotors is also one of the main targets to get better quality, modern computational method is used to determine strength and reliability characteristics. Generally the rotor dynamics is a main branch of engineering to studies the lateral and torsional vibrations of rotors with objective of expecting the rotor vibrations and containing the vibration level with acceptable limitations, the main components of a rotor dynamic system are the shaft of rotor with disk, the bearings and the seals, the shaft with the disk is the rotating part of the system **Nagaraju and Srinivas, 2014**.

Basically there are three types of vibrations associated with the motion of the rotor, axial, torsional and lateral vibrations. The axial vibration is the dynamics of the rotor in the axial direction while torsional vibration is the dynamics of the shaft in the rotational direction, basically this is very little influenced by the bearings that support the rotor and that is not a major problem, lateral vibration, the primary concern is the vibration of the rotor in lateral directions, **Abdul Ghaffar, at al., 2010**.

The bearings could be regarded as important parts in finding the lateral vibrations of the rotor, we will investigate the basic concepts of lateral dynamics of the rotor, with ever increase in demand for large size and speed in modern machines, rotor dynamics becomes more important in the mechanical engineering design. It is famous that torsional vibration in rotating machines, reciprocating machines installation and geared system, whirling of rotating shaft, the effect of flexible bearing, instability because of asymmetric cross-section shafts, hydrodynamics bearings, hysteresis, balancing of rotor can be understood only on the basis of rotor dynamics studies. Rotor dynamics is an important branch of the discipline of dynamics that pertains to the behavior of a huge assortment of rotary machines, **Maurice, 2010**. The aim of a standard rotor dynamics analysis and design checking is to help to characterize the transverse dynamic design characteristics but analysis of some rotary equipment may need analysis specific to the unit, a general method has used for performing the standard lateral analysis of vibration by using FEA with selected BEAM188 element for shaft and COMBI214 element for bearings in the ANSYS software.

2. FUNDAMENTAL EQUATIONS

2.1 Fluid Film Bearings

There are many parameters and physics phenomena that control the rotors apart from stationary structures but the main differences is the fluid film supports if we want to

understand the rotor dynamics as in **Fig.1**, In the past they were believe that the lubricant in the cavity of the bearing will decrease the friction and minimize the losses, and then they discovered that the fluid film doing many things more than the losses of the friction. If looking at **Fig.2**, the bearing center C and the journal center \tilde{C} will form an attitude of the bearing and makes the angle α with the vertical load (W), the clearance h will varying between two values.

From the bearing geometry and speed, eccentricity, pressure and attitude angle Sommerfeld derived such parameter to give an indication about the bearing eccentricity as, **Michael, et al.,2012**.

$$S = \frac{\mu DLN}{W} * \left(\frac{r}{h}\right)^2 \quad (1)$$

The radial and tangential forces F_r, F_t is

$$F_r = -\frac{D\Omega\mu L^3\epsilon^2}{2h^2(1-\epsilon^2)^2} \text{ and } F_t = -\frac{\pi D\Omega\mu L^3\epsilon}{8h^2(1-\epsilon^2)^{3/2}} \quad (2)$$

The force F_t opposes the sliding motion so that the power dissipation $F_t * \Omega D/2$, the resultant force on the bearing must be opposite to the load applied to the rotor.

$$F = \sqrt{F_r^2 + F_t^2} = \frac{\pi D\Omega\mu L^3\epsilon}{8h^2(1-\epsilon^2)^2} \left(\left(\frac{16}{\pi^2} - 1\right)\epsilon^2 + 1\right)^{1/2} \quad (3)$$

If the load on bearing is known then the modified Sommerfeld number is given by **Yukio and Toshio, 2012**.

$$S_s = \frac{D\Omega\mu L^3}{8fh^2} \quad (4)$$

These forces F_r and F_t are applied on both bearing bush and the journal, the tangential force F_t opposes the sliding motion so that the power dissipation is $F_t \Omega D/2$.The resultant force on the rotor (through the bush) must be equal and opposite to the load applied on the rotor, from Eq. (2), the magnitude of the resultant force as in Eq. (3), a vertical resultant force is common, where the load is due to the rotor weight; in this case, the position the journal takes in the bearing ensures that the load is indeed vertical. If the magnitude of this load is known, then the bearing eccentricity may be obtained by rearranging Eq. (3) to give Eq. (5), where S_s from Eq. (4) is called modified Sommerfeld number or Ocvirk number and is known for a particular speed, load, and oil viscosity, **Michael, et al.,2012**.

$$\epsilon^8 - 4\epsilon^6 + (6 - S_s^2(16 - \pi^2))\epsilon^4 - (4 + \pi^2 S_s^2)\epsilon^2 + 1 = 0 \quad (5)$$

The values of eccentricity ratio ϵ is equal $\frac{\bar{c}-c}{h}$ always taken between 0-1 so the value of ϵ has been found by iteration method from 0 to 6000 RPM by computer program of MATLAB.

When a linear bearing model is used in machine, the displacement should be checked to be small because a linear analysis does not include any constraints on the displacement, we considered only short bearing so the matrices is 2×2 for stiffness and damping matrices could be found as , **Michael, et al.,2012**.

$$K = \frac{F}{h} \begin{bmatrix} a_{xx} & a_{xy} \\ a_{yx} & a_{yy} \end{bmatrix} = \begin{bmatrix} K_{xx} & K_{xy} \\ K_{yx} & K_{yy} \end{bmatrix} \quad (6)$$

$$c = F/(h \times \Omega) \begin{bmatrix} b_{xx} & b_{xy} \\ b_{yx} & b_{yy} \end{bmatrix} = \begin{bmatrix} c_{xx} & c_{xy} \\ c_{yx} & c_{yy} \end{bmatrix} \quad (7)$$

$$\text{Where } h_0 = \frac{1}{(\pi^2(1-\varepsilon^2)+16\varepsilon^2)^{3/2}} \quad (8)$$

$$a_{xx} = h_0 \times 4(\pi^2(2 - \varepsilon^2) + 16\varepsilon^2) \quad (9)$$

$$a_{xy} = h_0 \times \frac{\pi((\pi^2(1-\varepsilon^2)^2)-16\varepsilon^4)}{\varepsilon\sqrt{1-\varepsilon^2}} \quad (10)$$

$$a_{yx} = -h_0 \times \frac{\pi(\pi^2(1-\varepsilon^2)(1+2\varepsilon^2)+32\varepsilon^2(1+\varepsilon^2))}{\varepsilon\sqrt{1-\varepsilon^2}} \quad (11)$$

$$a_{yy} = h_0 \times 4(\pi^2(1 + 2\varepsilon^2) + \frac{32\varepsilon^2(1+\varepsilon^2)}{(1-\varepsilon^2)}) \quad (12)$$

$$b_{xx} = h_0 \times \frac{2\pi\sqrt{1-\varepsilon^2}(\pi^2(1+2\varepsilon^2)-16\varepsilon^2)}{\varepsilon} \quad (13)$$

$$b_{xy} = b_{yx} = -h_0 \times 8(\pi^2(1 + 2\varepsilon^2) - 16\varepsilon^2) \quad (14)$$

$$b_{yy} = h_0 \times \frac{2\pi((\pi^2(1-\varepsilon^2)^2)+48\varepsilon^2)}{\varepsilon\sqrt{1-\varepsilon^2}} \quad (15)$$

The stiffness matrix is not symmetric, therefore, hydrodynamic bearings is anisotropic supports in to the machine. The MATLAB computer program has been designed to study the relations between eccentricity and modified Sommerfeld number, then getting the relation between modified Sommerfeld number and stiffness and Sommerfeld with damping. We take in to account the effect of dynamic forces acting on the bearings, generally the force-displacement relation is nonlinear but, its provided that amplitude of resultant is small, so can assume a linear force-displacement relation. We consider short bearing ($L/D < 1$), where the matrix are 2×2 , the stiffness and damping matrices may be written in closed form in term of eccentricity and load as shown in Eqs.(6) and (7). The representation of spring and damper of COMBI214 is 2-dimensions element with longitudinal tension and compression capability as shown in **Fig.3**.

2.2 Dynamic Equations

The concept of rotor dynamics has demonstrated by using the rotor which has disk lies at an equal distance from bearings, the bearings that taken with the rotor is short journal bearing $L < D$ and $A \neq B$ as shown in **Fig. 1**

The rotor consists of long flexible shaft with flexible journal bearing on both ends the bearings has support stiffness K_{xx}, K_{yy}, K_{xy} and K_{yx} associated with damping c_{xx}, c_{yy}, c_{xy} and c_{yx} .

in both ends in bearing 1 and bearing 2 as shown in **Fig.3**, there is a disk of mass m_d and the mass of shaft is m_s , the equivalent mass of the rotor is, **Michael, et al.,2012**.

$$m = m_d + \frac{17}{35} m_s \quad (16)$$

The center of gravity of disk is offset from the shaft geometry center by an eccentricity e , the motion of disk center is described by two translational displacements (x_r, y_r) .

The main form of equation of motion for all vibration problems is given by **Xu, et al, 2004**.

$$[m]\{\ddot{y}_r\} + ([c] + [cg])\{\dot{y}_j\} + ([K] + [H])\{y_j\} = \{f\} \quad (17)$$

Where

$[m]$ = symmetric mass matrix, $[c]$ = symmetric damping matrix, $[K]$ = symmetric stiffness matrix, $\{f\}$ = external force vector, $\{y\}$ = generalized coordinate vector.

The Eq. (17) is for motion a symmetric rotor and rotates at constant speed Ω about its spin axis but it is accompanied by skew symmetric gyroscopic matrix $[Cg]$ and skew symmetric circulatory matrix $[H]$. Both of $[Cg]$ and $[H]$ matrices are affected by rotational speed Ω . When the speed Ω is zero, the $[Cg]$ and $[H]$ in Eq. (17) vanished represents an ordinary stand still structure, the $[Cg]$ matrix has inertia terms and derived from kinetic energy because of the gyroscopic moments acting on the rotary parts of the machine, if this equation is described in rotary reference body this gyroscopic matrix $[Cg]$ Also has the terms which associated with Coriolis acceleration. The circulatory matrix $[H]$ is come mainly from internal damping of rotating elements, **Nagaraju and Srinivas, 2014**.

From Newton's second law of motion in x and y directions to get the equations of motion including the stiffness and damping of bearings

$$\sum F_x = m\ddot{x} \quad (18)$$

$$\sum F_y = m\ddot{y} \quad (19)$$

$$(K_x + K_{xx1} + K_{xx2})X_j + (K_{yx1} + K_{yx2})y_j + (c_{xx1} + c_{xx2})\dot{X}_j + (c_{xy1} + c_{xy2})\dot{y}_j - K_{xr} = m \frac{d^2}{dt^2} (X_j + e \cos(\Omega t + \Phi e)) \quad (20)$$

$$(K_{xy1} + K_{xy2})X_j + (K_{yy1} + K_{yy2} + K)y_j + (c_{xy1} + c_{xy2})\dot{X}_j + (c_{yy1} + c_{yy2})\dot{y}_j - K_{yr} = m \frac{d^2}{dt^2} (y_j + e \sin(\Omega t + \Phi e)) \quad (21)$$

Where Φe is the phase angle of mass unbalance, the above equations of motion gives indications about the motions in x and y directions are both decoupled in case of static and dynamic for this model therefore they can be solved separately to find response amplitude in x and y directions at any time.

2.3 Modeling and Design Data Input

The modeling features for rotor and bearing support flexibility are described in this papers and show how element BEAM188, COMBI214 are used to model the shaft with bearings and MASS21 for disk to model the masses. The stiffness and damping of both bearings with cross coupling directions and stiffness with damping of the shaft has been taken into account in this analysis including their variations with the changing of rotational spin speed to get accurate results. Beam element (BEAM188) is good for analyzing slender to moderately stubby or thick beam structures, it is a linear (2 –nodes) as shown in **Fig.4**, beam188 element has six or seven degrees of freedom at each node, with the number of degrees of freedom depending on the KEYOPT(1) value, when KEYOPT(1) = 0 at each node, these include translations in the x, y and z directions and rotations about x, y and z axes, when KEYOPT(1) = 1, a seven degree of freedom (warping magnitude) is also considered, this element is well suited for linear large relation and/or large strain nonlinear applications, MASS21 element for lamped mass disk is a point element having up to six degree of freedom displacement in x, y, z directions and rotation about x, y and z axes. A different mass and rotary inertia may be assigned to each coordinate direction, **Nagaraju and Srinivas, 2014**.

Tables 1 and **2** represent the values of stiffness and damping of bearings with the variations of spin speed so can represent the COMBI214 element in ANSYS for each bearing and at any speed, the results are from MATLAB program which has been designed to solve a set of equations from Eqs. (1) to (15). The values of damping coefficients decreased with rotational speed till to 2000 RPM then its change very small and its approximately considered constant values but the cross coupling values continue decreasing while the stiffness also change rapidly till to 2000, is seem stable and stiffness in cross coupling directions is not equal and varied small amounts as shown in **Figs. (5)** and **(6)**.

3. RESULTS AND DISCUSSION

Modal analysis without any rotation is performed on the rotor model. The Eigen frequency obtained for the rotor model at 0 RPM are drawn in **Fig. 7** which shows first mode shape of operation 6000 rpm by ANSYS, **Table 4** shows the dimension of the selected model ($A \neq B$). For Critical Speed and Campbell Diagram, In this analysis, the first

Eigen frequency analysis are done on the rotor model for speed range from 0 to 6000 rpm with an increment of 100 rpm using multiple load step, the fundamental Eigen frequency of the rotor model corresponding to different rotational spin speeds are plotted in Campbell diagram with limitation of the stability of the rotor as shown in **Fig.8**.

The Campbell diagram is used to find critical speed of the system by ANSYS which is 4920 RPM, often rotor critical speed against natural frequency of the system, the rotor is supported by two tilting pad short bearings, stiffness and damping coefficients of bearings are varied with spin speed and in this case the natural frequency of the system are varied, if the natural frequency equal to rotating spin speed, the speed is called critical speed, as shown in Campbell diagram the stability limit at 80.4 Hz and it called threshold limit so if the frequency less than threshold, it mean under the purple color line and the system is stable, if the frequency more than threshold, it mean up the purple color line and the system is stable too, if the frequency is 80.4 it mean, it is on the purple color line and the system is unstable.

For the harmonic analysis it has been showed that the unbalance response of the rotor at the disk location by apply the unbalance forces at the center position to get the displacement which vary sinusoidal at the same know frequency domain then the comparison has been done by changing the value of unbalance masses (0.5g, 1g, 1.5g, 2g and 2.5g) as shown in **Table 5**, to understand its effect on the rotor while its operating, it can be conclude that by increasing the unbalance masses, the displacement will also increase at the disk region and the relation between them shown in **Fig.13**, the unbalance harmonic response shown in **Figs. 9, 10, 11, 12, 13 and 14**. The maximum displacement happens at the critical speed case, the dynamic amplitude plotted against the unbalance mass as shown in **Fig.15**, the amplitude vary nonlinear till to 1g unbalance mass then it varies approximately linear after 1g to 2.5g.

For the transient analysis at start up, the response of the rotor system at the disk region to arbitrary time-varying load to find the stability of the system at different spin speeds, if the amplitude of the rotor decrease with the time, that means the system is stable otherwise the system is not stable. Also the values like rise time (t_r), overshoot (PM), settling time (t_s) has been calculated for transient start up case with changing the speed from 0 to 6000 rpm and for (0.5g, 1g, 1.5g, 2g, and 2.5g) unbalance mass as listed in **Table 6**, the transient has been compared just only as a behavior of the curves with **Ignacio, et al, 2013**, the comparison also has been done just only for understanding the behavior of curve for transient bending stress in z and y directions with **Ignacio, et al, 2013**. where blue color is bending stress in y direction and red color is bending stress in z direction, the maximum stress in y direction is $\mp 90E6 \frac{N}{m^2}$, while in z direction the maximum stress $\mp 62E6 \frac{N}{m^2}$, both of them happens at 6.55sec. the behaviors were in good agreement if compare with transient stress as in **Ignacio, et al, 2013** as shown in **Figs.16, 17, 18, 19, 20 and 21** for displacement and **Figs.22 and 23** for bending stress for a rotor has 1g unbalance mass.



4. CONCLUSION

It can be conclude that.

- 1- The Eigen frequency calculated as a first critical speed by ANSYS, to get the fundamental frequency and mode shape by using Campbell diagram which is the resonance speed, it found 4920 rpm for a given dimensions of rotor as in **Table.4**, resonance speed is more dangerous case to avoid it by making its period of time as small as possible to avoid failure.
- 2- The harmonic analysis has been taken for many unbalance masses 0.5g to 2.5g (step 0.5g) and finding the response for each case, the peak value of response happen at 80.4 Hz on frequency-response relation and also could be conclude that the unbalance response varies nonlinear with unbalance mass till to 1g then it became approximately linear variation with unbalance masses from 1g to 2.5g.
- 3- The transient response and transient bending stresses has been studied and compared as a behavior of curve, it found in good agreement, the rise time changed from 0.2% - 1% as increasing percentage from 0.5g to 2 g while its 20% increasing if change from 2g to 2.5g but the overshoot not varies so much, the settling time jumped to 8.312 sec. at 2.5g unbalance mass, the peak response of transient case also increases by increasing the unbalance mass, from the other hand the bending stress in y-direction is more than in z-direction and the maximum case of response and stresses happen at 6.55sec. the transient response and stresses has been compared as a behavior of curves with **Ignacio, et al, 2013**, it found in good agreements.

REFERENCES

- Abdul Ghaffar Abdul Rahman, Ong Zhi Chao and Zubaidah Ismail, 2010, *Effectiveness of Impact-Synchronous Time Averaging in Determination of Dynamic Characteristics of a Rotor Dynamic System*, Technical Paper, Mechanical Engineering Department, Faculty of Engineering, University of Malaya, 50603 Kuala Lumpur, Malaysia.
- Chen Y. S , Cheng Y. D , Liao J. J and Chiou C. C, 2008, *Development of A Finite Element Solution Module for the Analysis of the Dynamic Behavior and Balancing Effects of an Induction Motor System*, Technical Paper, Department of Mechanical Engineering, Yuan-Ze University, Chungli 320 Taiwan, ROC.
- Ignacio Ramirez Vargas, Luis Manuel Palacios Pineda, and Humberto Corro Hernandez, 2013, *Vibrational Response of a Rotor Supported in Hydrodynamics Short Bearings*, Memories Del Xix International Congress of Her Annual Somim, 25 Al 27 De September, 2013 PACHUCA, HIDALGO, MEXICO.

Kris Matthys, Marco Perucchi and Koenraad De Bauw, *Rotor Dynamic modeling as powerful support tool for vibration Analysis on large Turbo machinery.* ○



- Maurice L, Adams, 2001, *Rotating Machinery Vibration*, From analysis to Troubleshooting, Marcel Dekker, Inc.
- Michael, I. Friswell., John E. T. Penny, and Arthur W. Lees, 2012 , *Dynamics of Rotating Machines*, Cambridge University Press, 32 Avenue of the Americas New York NY 10013-2473 USA, First Published 2010, Reprinted 2012, pp177-183.
- Nagaraju Tena and Srinivas Kadivendi, 2014, *Rotor Dynamic Analysis of Steam Turbine Rotor Using ANSYS*. IJMERR, ISSN2278-0149, Vol.3, No1.
- Xu Yang, Zhao Lei and Yu Suyuan, 2004, *Dynamics Analysis of Very Flexible Rotor* ,Technical Paper, Institute of Nuclear Energy Technology, Tsinghua University, Beijing 100084, P.R.China.
- Yukio Ishida and Toshio Yamamoto, 2012, *Linear and Nonlinear Rotor Dynamics,(A Modern Treatment with Applications*, 2nd Enlarged and Improved Edition, Wiley-VCH Verlag, Germany, pp307-320.

NUMENCLATURE

- a_{xx} = factor of stiffness of bearing in x-direction.
 a_{xy} = factor of cross coupling stiffness of bearing in xy-direction.
 a_{yx} = factor of cross coupling stiffness of bearing in yx-direction.
 a_{yy} = factor of stiffness of bearing in y-direction.
 b_{xx} = damping parameter of bearing in x-direction.
 b_{xy} = cross coupling damping parameter in xy-direction.
 b_{yx} = cross coupling damping parameter in yx-direction.
 b_{yy} = damping parameter of bearing in y-direction.
 C = center of bearing.
 \tilde{C} = center of journal.
 c_{xx} = damping of bearing in x-direction, N.s/m
 c_{xy} = cross coupling damping of bearing in xy-direction, N.s/m
 c_{yx} = cross coupling damping of bearing in yx-direction, N.s/m
 c_{yy} = damping of bearing in y-direction, N.s/m
 D_s = shaft diameter, m
 E = Young's modulus of elasticity, $\frac{N}{m^2}$
 F = resultant force in bearing, N
 F_r = radial force in bearing, N
 F_t = tangential force in bearing, N
 H = disk thickness, m
 h = clearance between shaft and bearing, m.
 K_{xx} = stiffness of bearing in x-direction, N /m
 K_{xy} = cross coupling stiffness of bearing in xy-direction, N /m



K_{yx} = cross coupling stiffness of bearing in yx-direction, N /m

K_{yy} = stiffness of bearing in y-direction, N /m

K_{yr} = stiffness of rotor in y-direction, N /m

L = length of journal bearing, m

m = equivalent mass of rotor, Kg

m_d = mass of disk, Kg

m_s = mass of shaft, Kg

N = rotational speed, RPM

O = center of shaft before rotation.

S = Sommerfeld number.

S_s = modified Sommerfeld number.

t = time, sec.

u = generalized coordinate with lateral direction.

w = weight effect on bearing, N

x, y, z coordinates of the rotor

π = constant, 22/7

ϵ = eccentricity ratio.

Ω = excitation angular velocity, rad/sec.

θ = angle of hydrodynamic pressure, rad.

μ = viscosity of oil of bearing,

φ = pressure angle of oil film bearing, rad.

ρ = mass density of shaft material, $\frac{Kg}{m^3}$

ϑ = Poisson's Ratio.

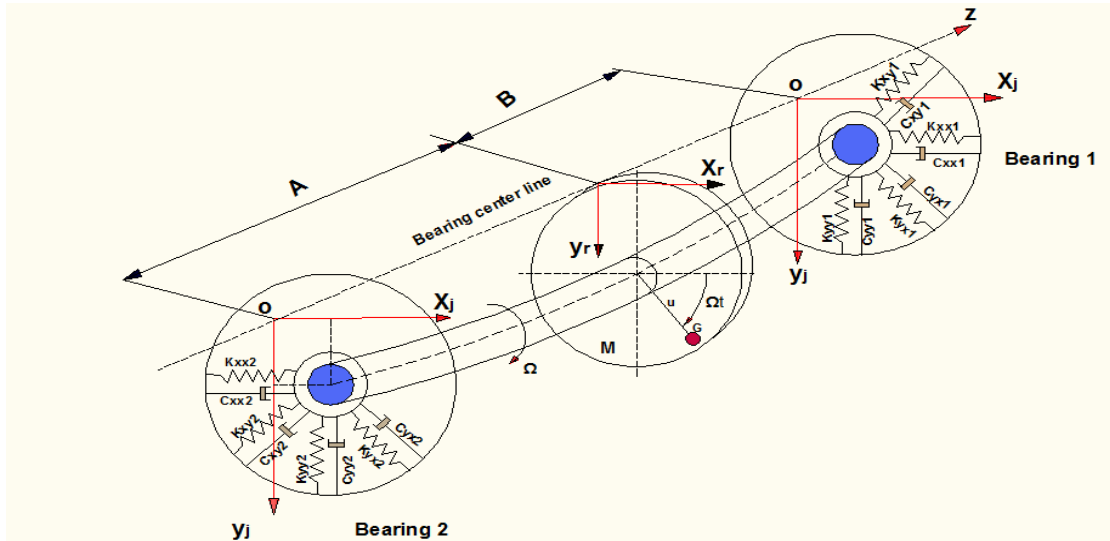


Figure 1. The bearings that taken with the rotor springs and damper representation.

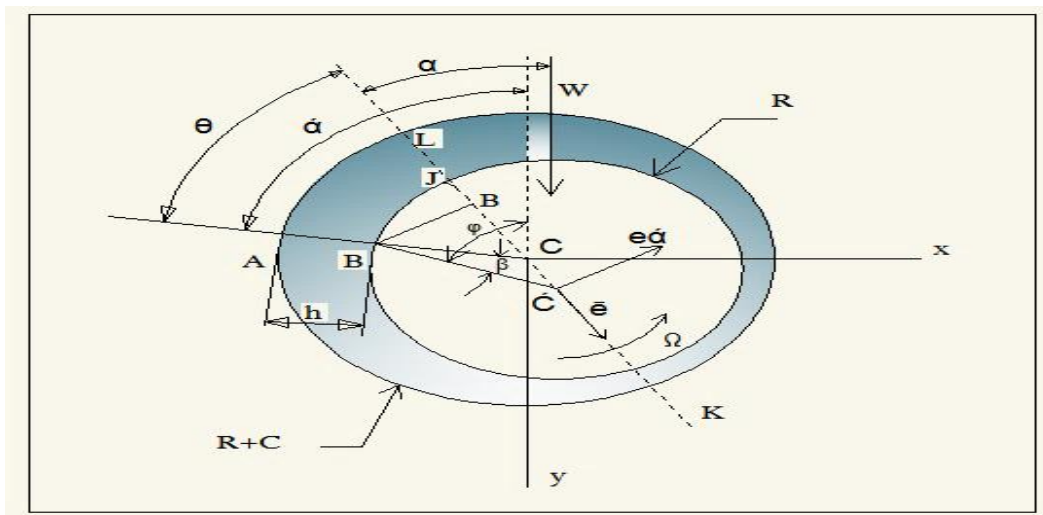


Figure 2. Fluid film bearing shows the eccentricity between shaft and bush.

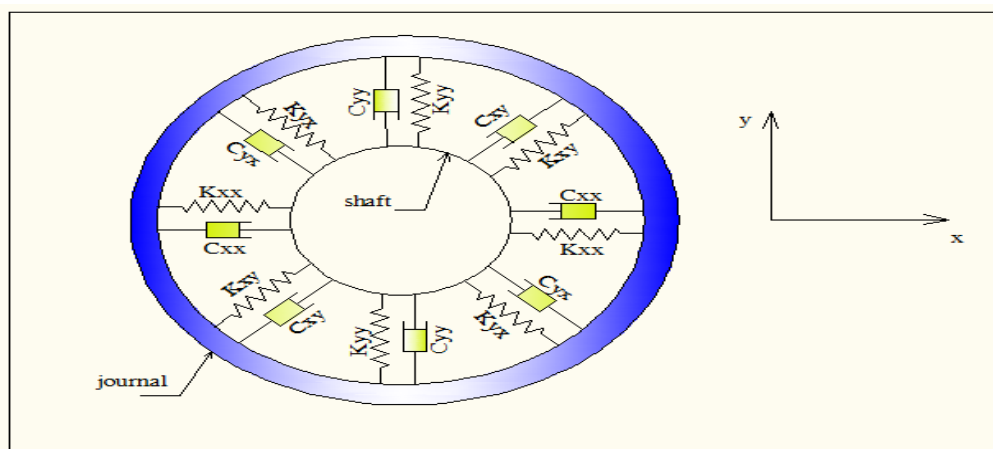


Figure 3. Springs and dampers with cross coupling of oil film journal bearing COMBI214 element geometry.

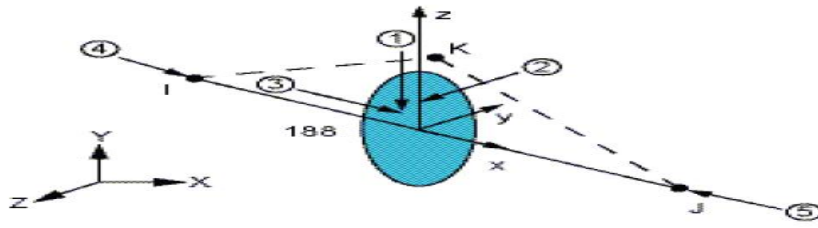


Figure 4. Element Beam 188 type 6 degree of freedom system, Kris, et al.,

Table 1. Properties of Bearing number 1, (Stiffness and damping).

Speed RPM	Eccentricity ratio	$K_{xx1}^* \cdot 10^3$	$K_{xy1}^* \cdot 10^3$	$K_{yx1}^* \cdot 10^3$	$K_{yy1}^* \cdot 10^3$	$c_{xx1}^* \cdot 10^3$	$c_{xy1}^* \cdot 10^3$	$c_{yx1}^* \cdot 10^3$	$c_{xx1}^* \cdot 10^3$
500	0.4419	3010	1646.8	-5273.5	3307.5	92.808	-58.21	-58.21	171.52
1000	0.2938	3199.2	3584.5	-5992.5	2345.2	78.512	-30.726	-30.726	104.39
1500	0.2158	3275.2	5448.3	-7221.7	2032.2	74.329	-20.916	-20.916	86.99
2000	0.1690	3311.0	7291.4	-8682.6	1895.6	72.552	-15.839	-15.839	79.988
2500	0.1382	3330.2	9133.1	-10272	1825.0	71.689	-12.737	-12.737	76.550
3000	0.1167	3341.4	10965	-11927	1784.4	71.157	-10.640	-10.640	74.581
3500	0.1008	3348.5	12804	-13636	1759.0	70.870	-9.1422	-9.1422	73.406
4000	0.0887	3353.2	14634	-15365	1742.2	70.641	-8.0095	-8.0095	72.593
4500	0.0791	3356.6	16475	-17128	1730.4	70.532	-7.1259	-7.1259	72.080
5000	0.0714	3359.0	18303	-18893	1721.9	70.411	-6.4174	-6.4174	71.668
5500	0.0650	3360.8	20149	-20685	1715.6	70.377	-5.8368	-5.8368	71.418
6000	0.0597	3362.2	21973	-22466	1710.7	70.288	-5.3523	-5.3523	71.165

Table 2. Properties of bearing number 2, (Stiffness and damping).

Speed RPM	Eccentricity ratio	$K_{xx2}^* \cdot 10^3$	$K_{xy2}^* \cdot 10^3$	$K_{yx2}^* \cdot 10^3$	$K_{yy2}^* \cdot 10^3$	$c_{xx2}^* \cdot 10^3$	$c_{xy2}^* \cdot 10^3$	$c_{yx2}^* \cdot 10^3$	$c_{xx2}^* \cdot 10^3$
500	0.3703	2251.4	1760.4	-3956.9	2008.4	85.47	-43.38	-43.38	132.91
1000	0.2289	2364.4	3663.7	-5025.7	1504.7	75.68	-22.658	-22.658	102.74
1500	0.1624	2401.8	5527.7	-6496.4	1361.4	73.096	-15.318	-15.318	79.99
2000	0.1249	2417.7	7385.5	-8131.4	1303.3	72.096	-11.556	-11.556	76.079
2500	0.1012	2425.7	9237.4	-9842.1	1274.7	71.588	-9.2718	-9.2718	74.169
3000	0.0849	2430.2	11094	-11601	1258.6	71.337	-7.739	-7.739	73.142
3500	0.0731	2433.0	12944	-13381	1248.7	71.156	-6.6406	-6.6406	72.488
4000	0.0641	2434.9	14806	-15189	1242.2	71.069	-5.8144	-5.8144	72.118
4500	0.0571	2436.1	16655	-16997	1237.7	71.007	-5.1708	-5.1708	71.817
5000	0.0515	2437.1	18494	-18802	1234.5	70.901	-4.6553	-4.6553	71.558
5500	0.0469	2437.7	20330	-20611	1232.1	70.811	-4.2331	-4.2331	71.355
6000	0.0430	2438.3	22193	-22450	1230.3	70.823	-3.8811	-3.8811	71.281



Table 3. Shaft material AISI4140 Properties.

Material Properties	
Young Modulus (E)	$2.05 \times 10^{11} \text{ N/m}^2$
Poisson's Ratio (ν)	0.29
Density (ρ)	7850 Kg/m^3

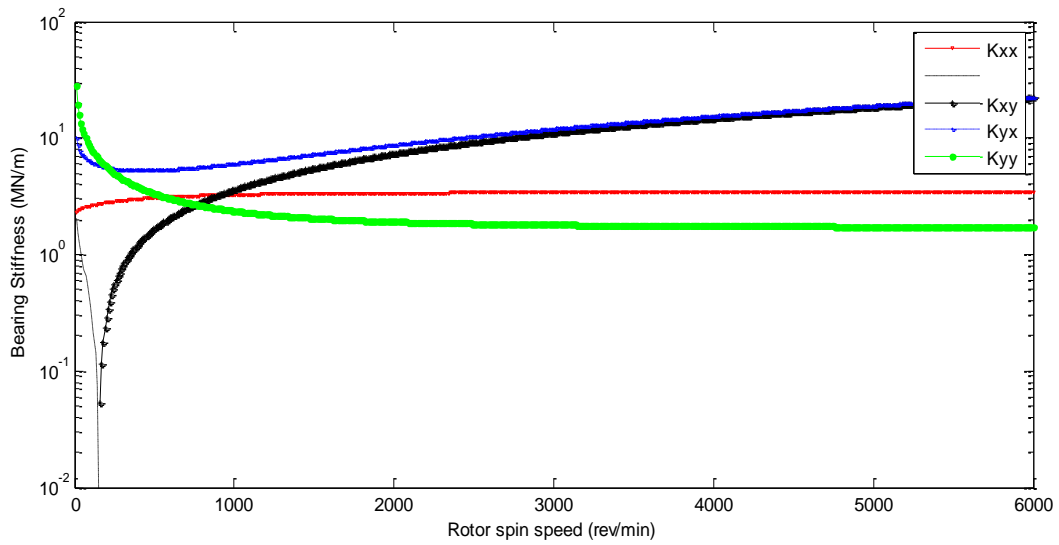


Figure 5. Stiffness of the journal bearing verses spin speed of rotor.

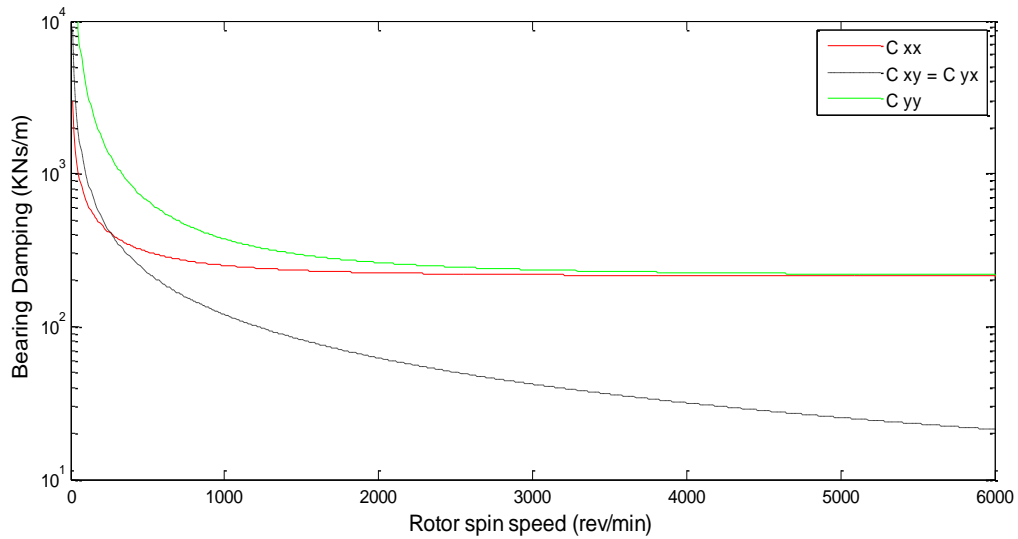


Figure 6. Rotor spin speed verses damping of fluid film bearing.

Table 4. Dimensions of Selected model For Study.

Description	Dimensions of selected model
Total shaft length (m)	0.654 m
Shaft diameter (m)	0.048 m
Disk diameter (m)	0.34 m
Distances between disk and bearings (m)	A=0.414m , B =0.24m
Disk thickness (m)	0.02m
Total rotor mass (Kg)	23.25 kg

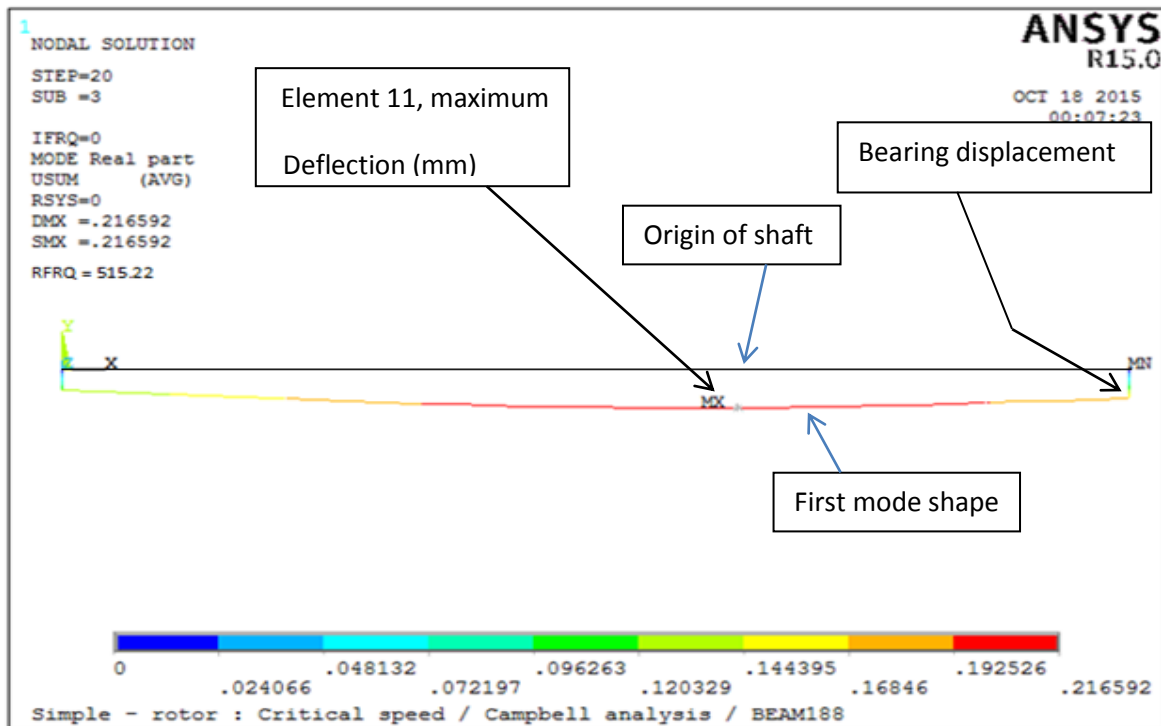


Figure 7. Mode shape of the rotor for first natural damped frequency.

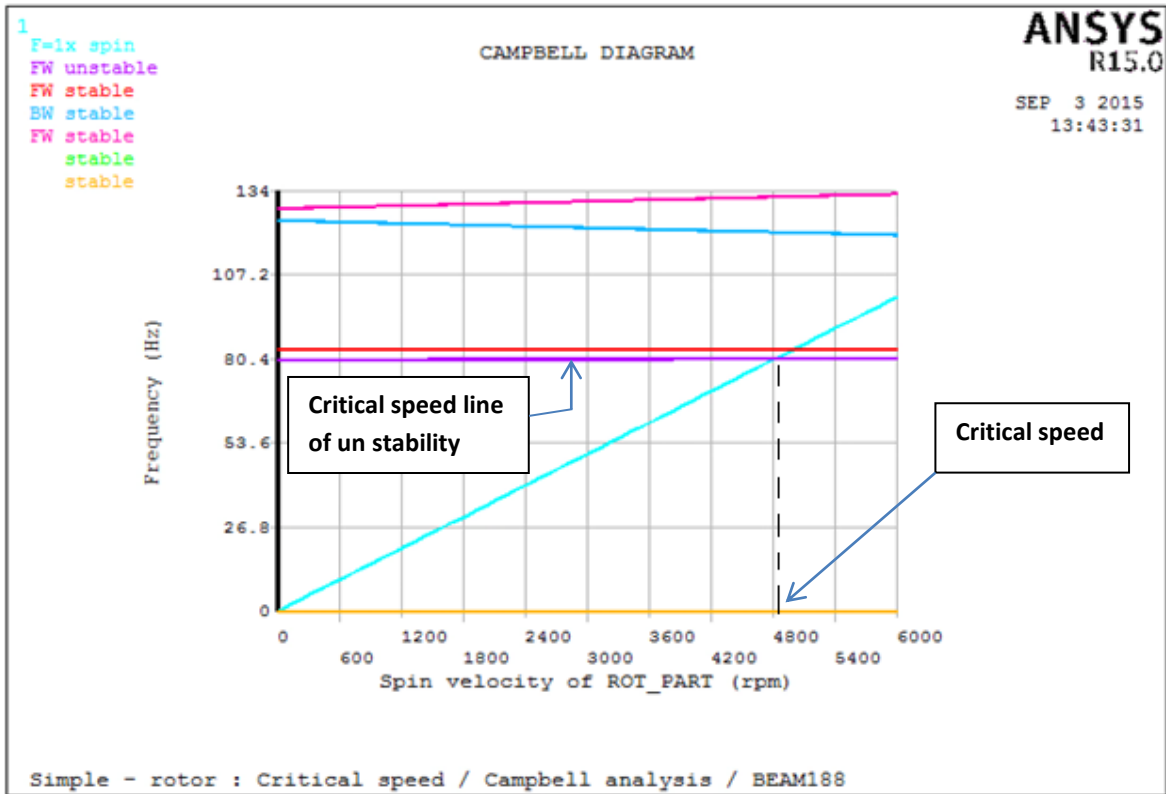


Figure 8. Campbell diagram of the rotor shows the critical speed at 4920 rpm.

Table 5. Response of the rotor in disk region of harmonic unbalance at critical speed.

Unbalance mass (g)	Response of the rotor in disk region (m) at 4920 rpm	% Percentage of changing response
0.5	0.7762E-03	0
1	0.8954E-03	13.31
1.5	0.1119E-02	19.98
2	0.1343E-02	16.67
2.5	0.1492E-02	9.986

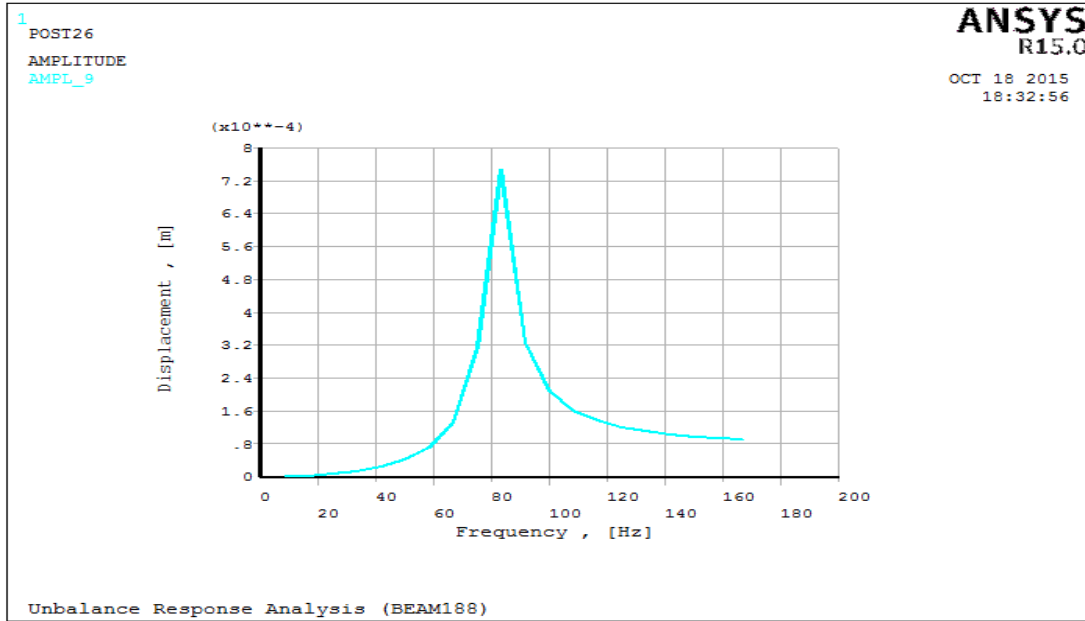


Figure 9. Response displacement for 0.5 g Harmonic unbalances mass.

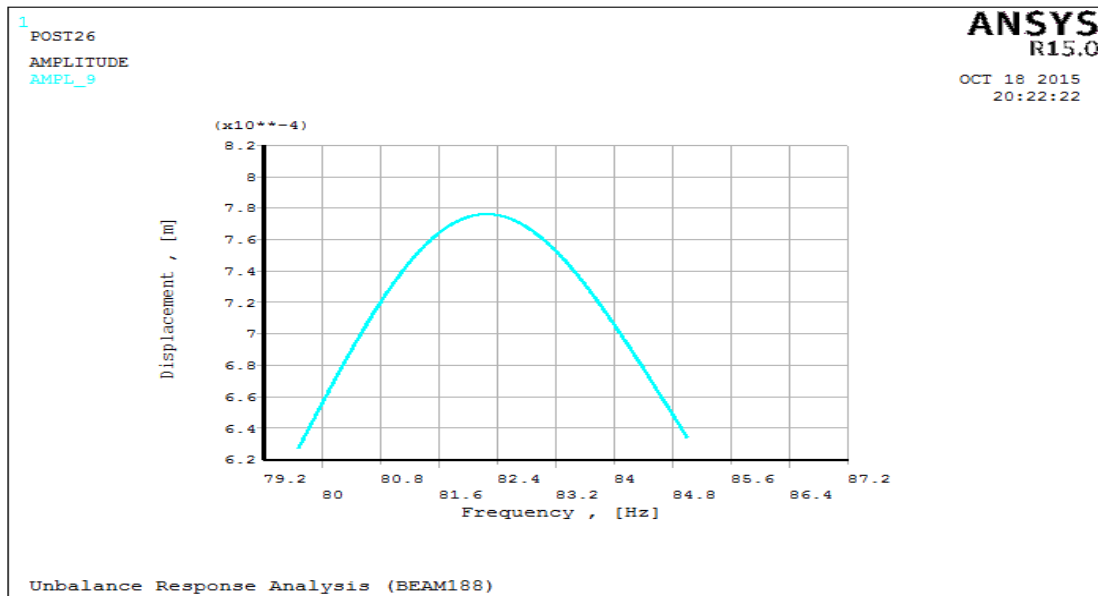


Figure 10. Response displacement for 0.5 g Harmonic unbalances mass, to show exact response value.

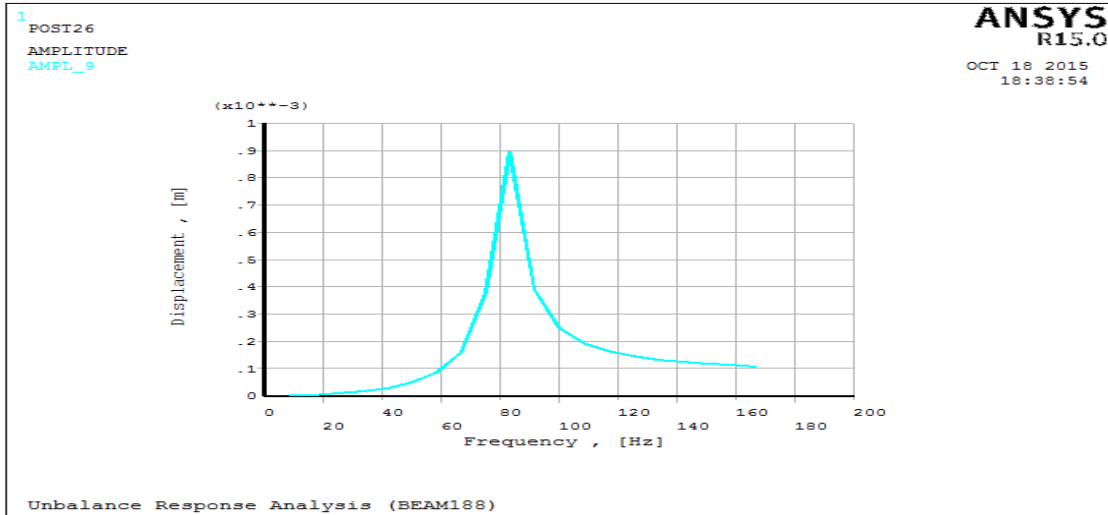


Figure 11. Response displacement for 1 g Harmonic unbalances mass.

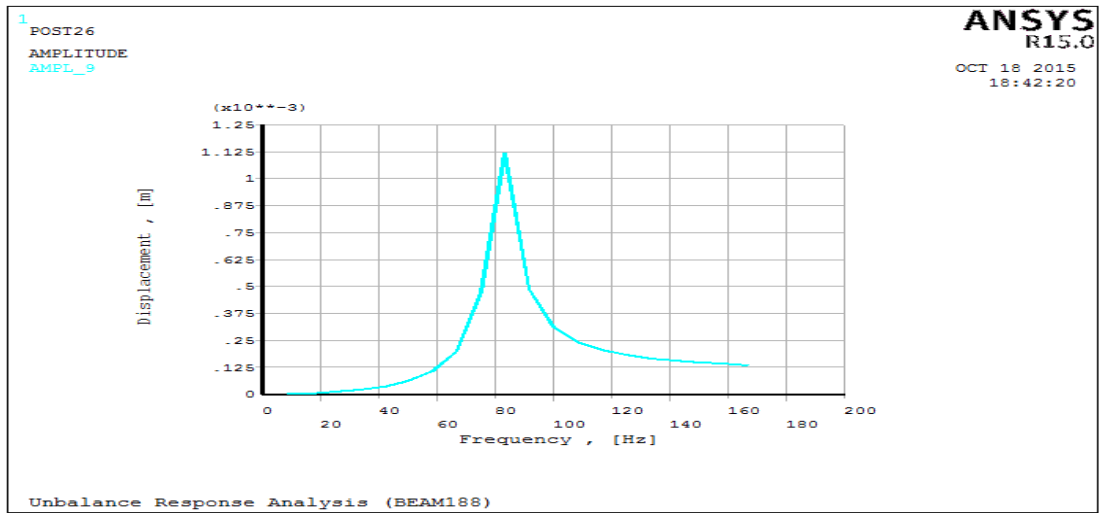


Figure 12. Response displacement for 1.5 g Harmonic unbalances mass.

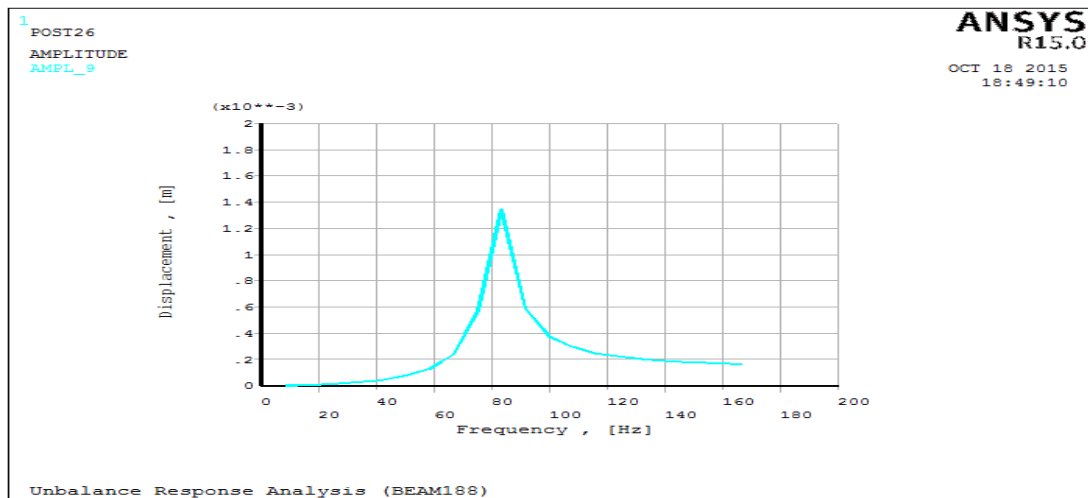


Figure 13. Response displacement for 2 g Harmonic unbalances mass.

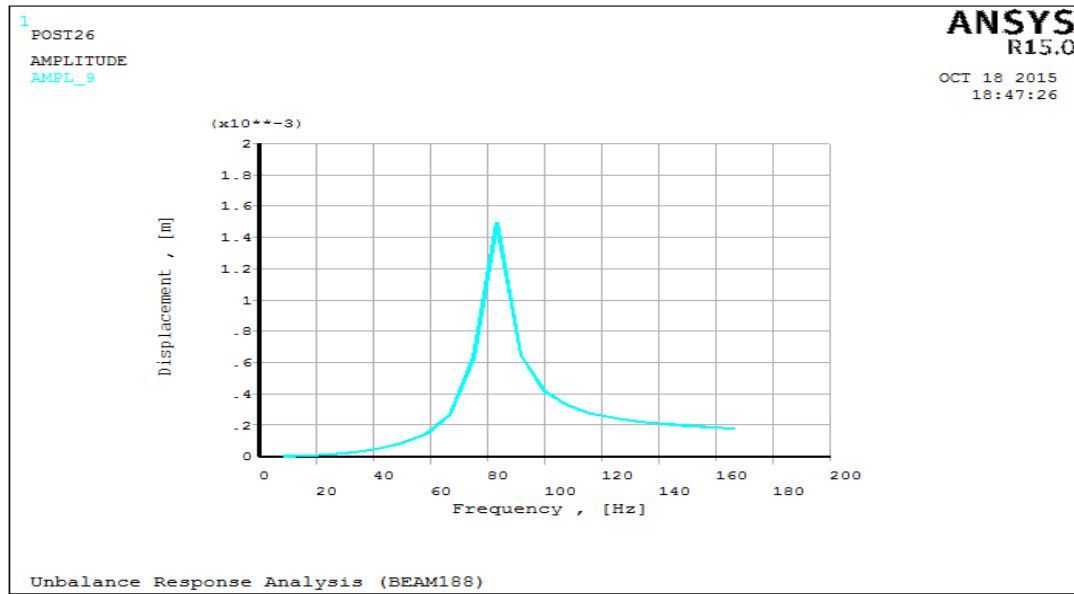


Figure 14. Response displacement for 2.5 g Harmonic unbalances mass.

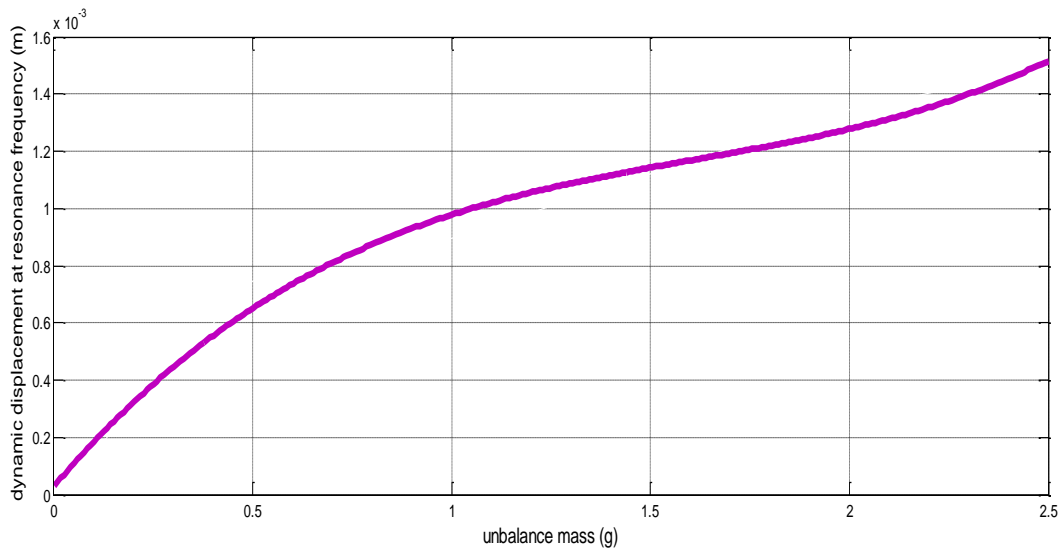


Figure 15. Response displacement versus unbalance mass at speed 4932 rpm.

Table 6. Transient response analysis at start up.

Transient analysis at start up for changes of unbalance mass					
Parameter	Time in second for 0.5g	Time in second for 1g	Time in second for 1.5g	Time in second for 2g	Time in second for 2.5g
Rise time t_r	6.172	6.187	6.253	6.285	7.9166
Settle time t_s	8.28	8.30	8.35	8.45	9.583
% overshoot MP	66.49	66.48	66.48	66.493	66.48
Maximum displacement near disk	0.7462E-03m at 6.478sec.	0.895E-03m at 6.50 sec.	0.1119E-02 m at 6.58 sec	0.1343E-02m at 6.650 sec.	0.1492E-2m at 8.312 sec.

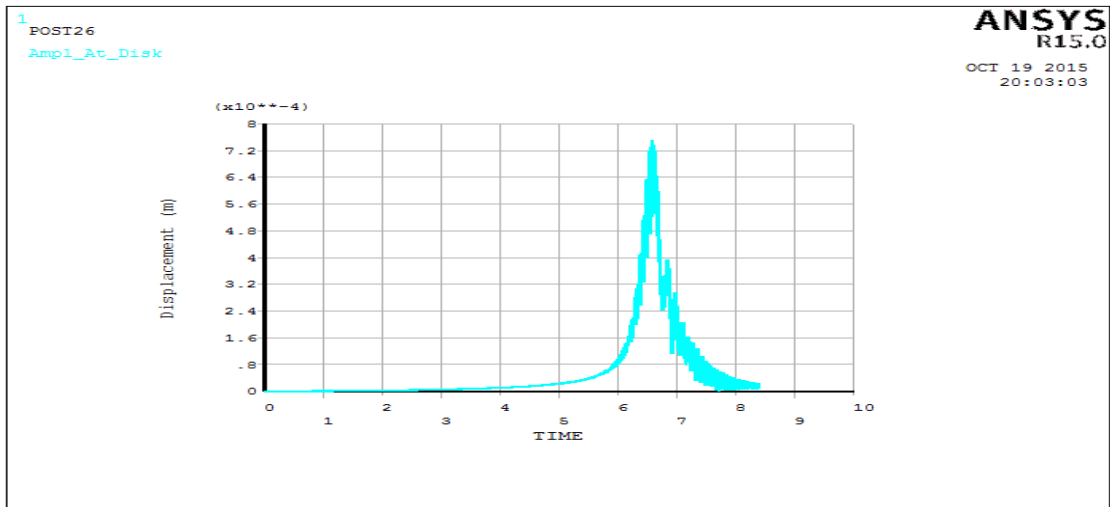


Figure 16. Transient Response Analysis Verses the Time for speed 0 to 6000 rpm with 0.5g unbalance mass.

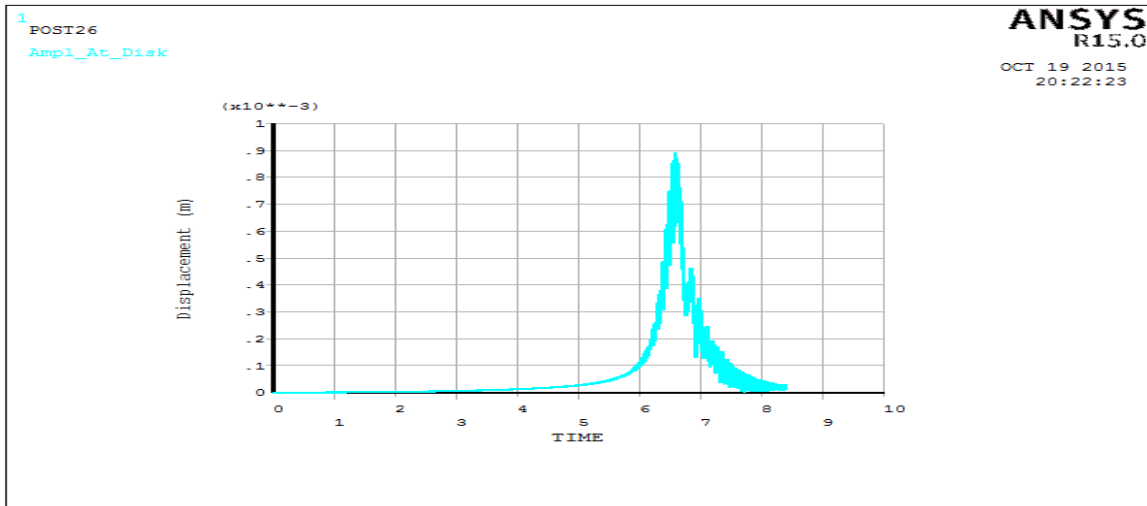


Figure 17. Transient Response Analysis Verses the Time for speed 0 to 6000 rpm with 1g unbalance mass.

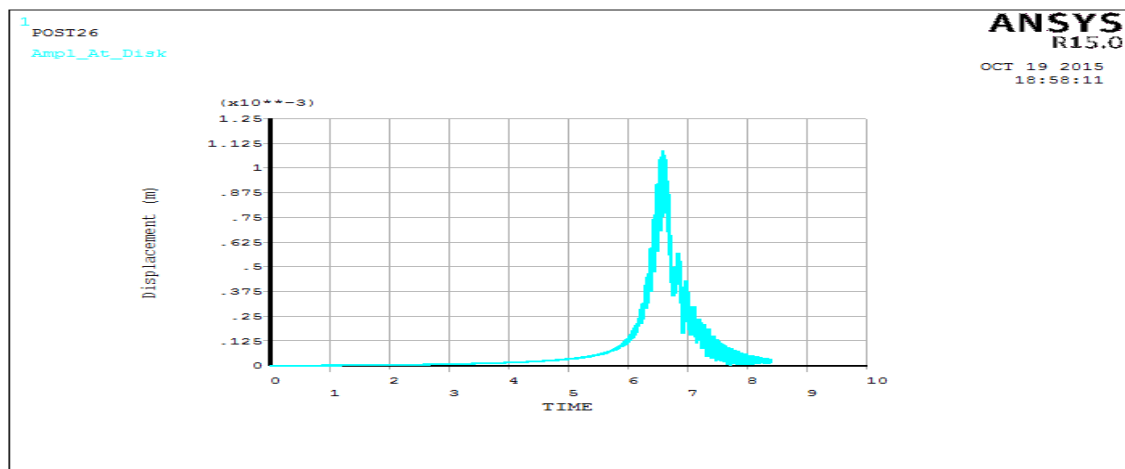


Figure 18. Transient Response Analysis Verses the Time for speed 0 to 6000 rpm with 1.5g unbalance mass.

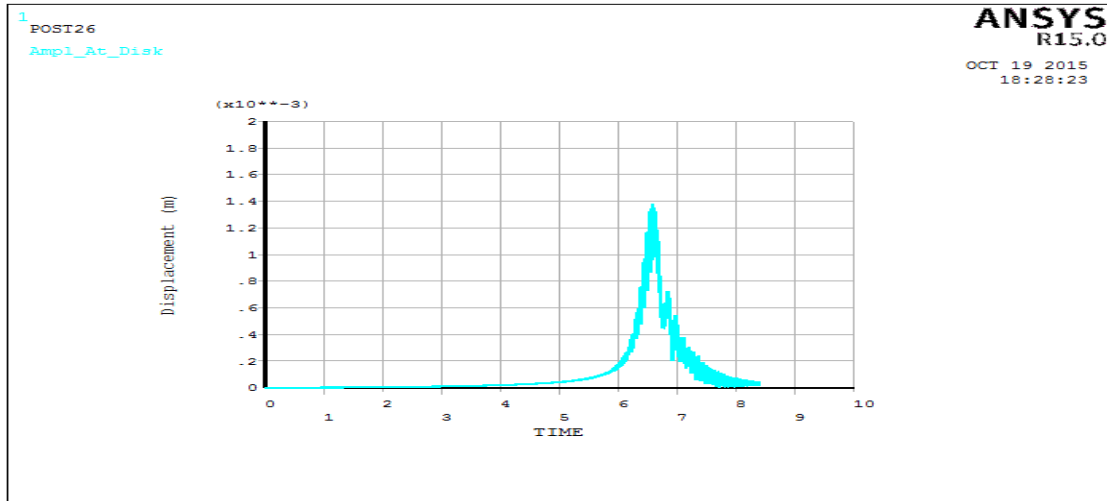


Figure 19. Transient Response Analysis Verses the Time for speed 0 to 6000 rpm with 2g unbalance mass.

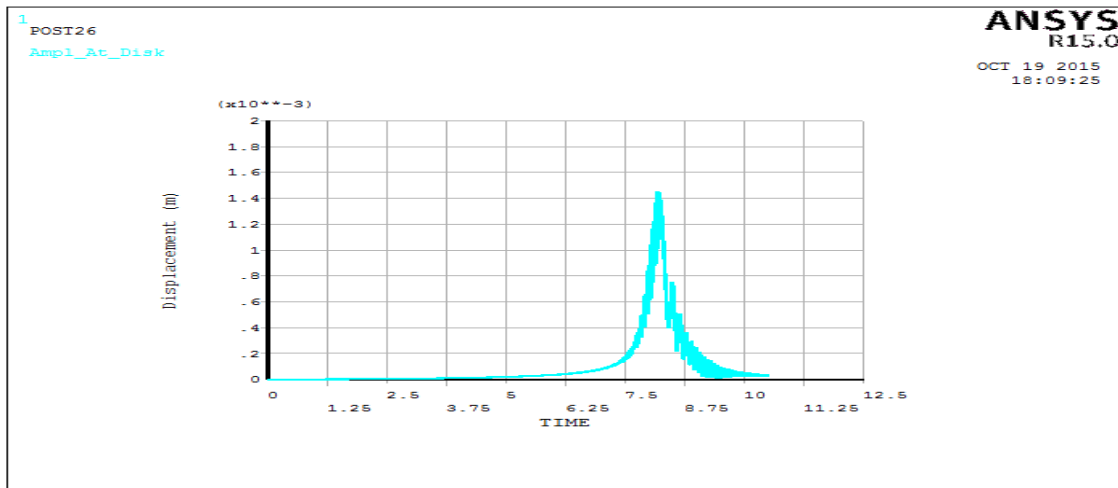


Figure 20. Transient response analysis versus the time for speed 0 to 6000 rpm with 2.5g unbalance mass.

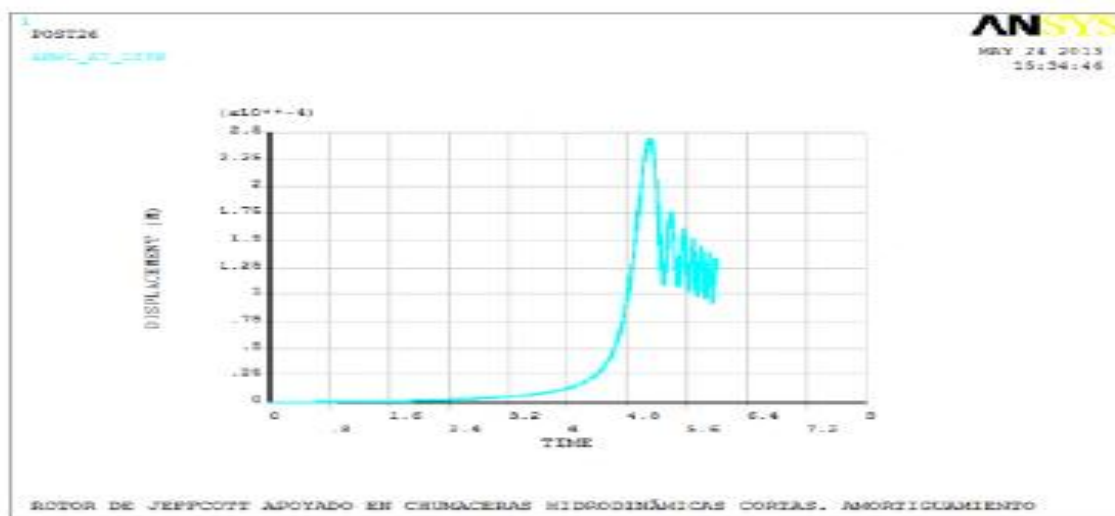


Figure 21. Transient response analysis versus the time as in, **Ignacio, et al., 2013.**

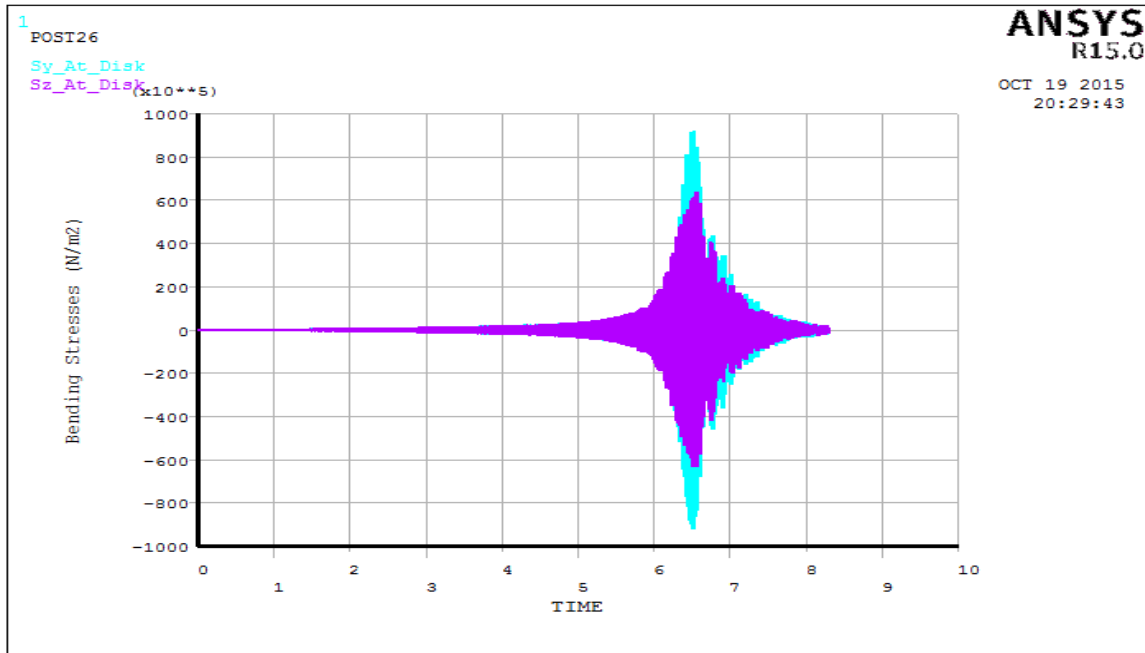


Figure 22. Bending stresses in z and y direction verses the time for transient at start up.

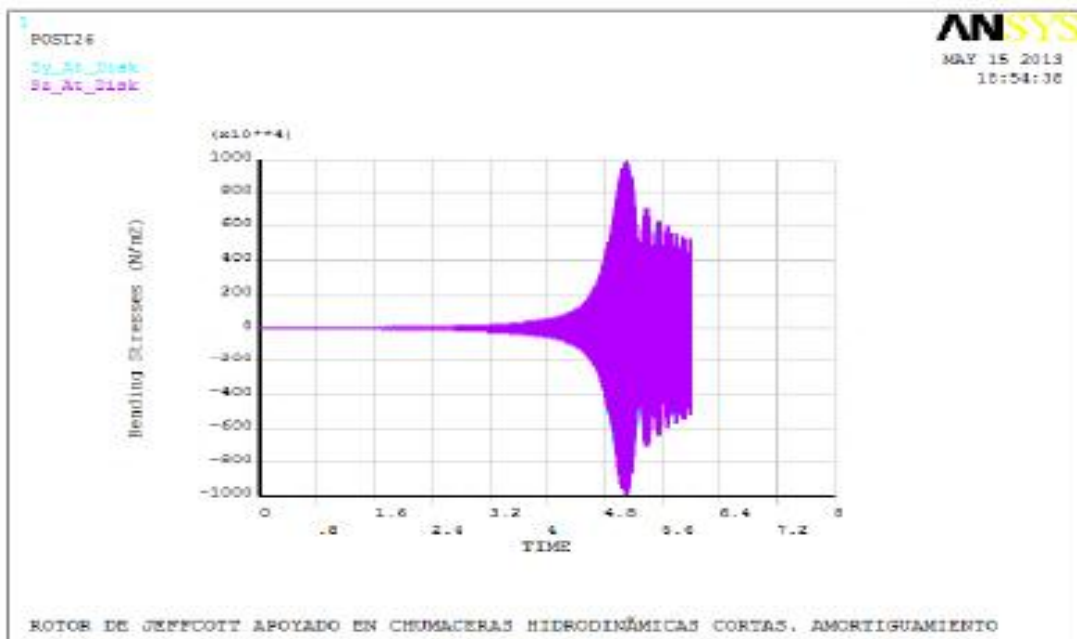


Figure 23: Bending stresses in z and y direction verses the time for transient at start up, **Ignacio, et al., 2013.**